J. Micropalaeontology, 41, 129–147, 2022
https://doi.org/10.5194/jm-41-129-2022

Journal of Micropalaeontology
Open Access

Meghalayan environmental evolution of the Thapsus coast (Tunisia) as inferred from sedimentological and micropaleontological proxies

Mohamed Kamoun[1], **Martin R. Langer**[2], **Chahira Zaibi**[1], **and Mohamed Ben Youssef**[3]

[1]GEOGLOB Laboratory, Sfax University, Faculty of Sciences of Sfax, BP 1171, 3000 Sfax, Tunisia
[2]Institut für Geowissenschaften, Paläontologie, Universität Bonn, Nussallee 8, 53115 Bonn, Germany
[3]Water Researches and Technologies Center, Borj Cedria, Tunisia

Correspondence: Mohamed Kamoun (med23km@yahoo.fr)

Received: 1 December 2021 – Revised: 13 June 2022 – Accepted: 25 June 2022 – Published: 13 September 2022

Abstract. Thapsus was one of the Roman Empire's largest harbors and is situated next to an easily defended promontory on Tunisia's coast in northern Africa. It was provided with a huge stone and cement breakwater mole that extended almost 1 km into the sea. We examined sedimentological and micropaleontological proxies from ^{14}C-dated core material and shifts in microfauna and macrofauna community structure to infer patterns of sediment dynamics and the chronology of events that shaped the coastal evolution in the Dzira Lagoon at Thapsus over the past 4000 years. The sedimentological and faunal record of environmental changes reflect a sequence of events that display a transition from an open to a semi-closed lagoon environment. At around 4070 cal yr BP and again between 2079 and 1280 cal yr BP, the data reveal two transgressive events and a deposition of sandy sediments in a largely open marine lagoon environment. The transgressive sands overlay marine carbonate sandstones that are upper Pleistocene in age. A gradual closure of the lagoon from 1280 cal yr BP until today is indicated by decreasing species richness values, lower abundances of typical marine taxa, and increasing percent abundances of fine-grained sediments. The environmental transition from an open to a closed lagoon setting was also favored by the construction of an extensive harbor breakwater mole, changes in longshore current drift patterns, and the formation of an extensive sand spit.

1 Introduction

The ancient city of Thapsus, situated on the east coast of Tunisia between Sousse and Sfax, was founded by the Phoenicians and served as a major trading hub between the Strait of Gibraltar and the Levant region of the eastern Mediterranean (Fig. 1a). Thapsus was established around Rass Dimass, a cape extending into the sea providing natural shelter for vessels and enabling safe anchorage for loading and discharge of cargo. When the Phoenicians fought against the Romans in the Punic Wars, Thapsus sided with Roman emperors (Gordianus I, II, II) and was fortified with an enormous harbor infrastructure, an amphitheater, and a huge breakwater mole (Davidson and Yorke, 2014). The massive concrete and stone breakwater structure extended almost 1 km into the sea (Fig. 1e) and represents one of the Roman Empire's longest harbor structures known to date (Dallas and Yorke, 1968; Yorke, 1967). Due to erosion by waves, pillaging for local house constructions, a rising sea level, and the erection of a small fishing port on top of the ancient harbor structure, only about 100 m of the original breakwater mole remains above water today (Slim et al., 2004).

In the north and current-protected lee of Rass Dimass and prior to the construction of the breakwater mole, the prevailing current drift action resulted in the formation of a long sand spit (Fig. 1b–c). Today, the sand spit is attached to the land and stretches over 4 km, with a width of 200 m, and forms a barrier (Dzira Island) composed of beaches and dunes that separates a shallow lagoon (Dzira Lagoon) from the open Monastir Bay. The extremity NW of the sand spit shows several hooks reflecting various stages of its development (Fig. 1c). In addition, between the Dzira sand spit and

Kuriat Island, several sand spits, shoals, and swash bars occur (Fig. 1f). The shallow lagoon served as a natural harbor during antiquity (Fig. 1e; Davidson and Yorke, 2014) and was illustrated in Andrea Palladio's 16th century treatise of the Battle of Thapsus (Fig. 1f; Giocondo and Palladio, 1567). At the southern entrance to the lagoon, a tidal channel, related to anthropogenic actions, allowed a connection with the open sea for several years before its recent clogging (Fig. 1c–d). The massive breakwater mole was built to add the existing natural shelter. However, dynamic coastal processes including littoral drift, lateral movements of sediments, and a rising sea level continued to shape the coastal habitats at Thapsus.

Within Monastir Bay, sediments settle in a comparatively protected environment, and along the shallow bay shore (0 to 2 m depth) the bottom is covered by medium sand. Sediment transport is mainly from north to south and vice versa, driven by longshore drift and rip currents. Both currents are generated by wind and swell, especially by north to northeast waves which transport the finest sediment.

Monastir Bay is characterized by wind speeds that range between 1 and 5 $m\,s^{-1}$. Prevailing wind directions are W, NNE, and E with occurrence probabilities of 10.7 %, 8.5 %, and 7.6 %, respectively (Souissi et al., 2014). Tides at Monastir Bay are semi-diurnal and generally of low amplitude. Average tidal ranges are 30 cm but occasionally reach 70 cm. Wind-induced currents are of the order of 5 to 10 $cm\,s^{-1}$. Over the entire Bay of Monastir and in particular around the Kuriat Islands, the predominant dynamic agent is swell. At the level of the Kuriat Islands, the coastal currents run along the series of shoals that link the Kuriat–Cogniliera archipelago with the shores of Teboulba.

In this study we provide high-resolution sedimentological and micropaleontological analyses of three radiocarbon-dated cores to reconstruct the coastal evolution around the ancient harbor of Thapsus. Our objectives were (1) to trace the environmental history of lagoonal habitats, (2) identify the impact of anthropogenic activities (breakwater mole construction) on coastal sediment dynamics, and (3) correlate major events with those recognized at other sites along the Mediterranean coast.

2 Materials and methods

To reconstruct the environmental evolution at Thapsus, a multi-proxy analysis was conducted on three cores (RD1, RD3, and RD8) recovered from the intertidal zone of Dzira Lagoon (for core locations see Fig. 1c). At the time of drilling, core areas for sites RD3 and RD8 were covered with 5 cm and for RD1 with 20 cm of water.

Cores were drilled with PVC (polyvinyl chloride) tube coring devices (core diameter 60 mm). In the laboratory, cores were cut in half longitudinally, photographed, and analyzed for sediment types, grain size, texture, structure, color, organic constituents, and microfossil and macrofossil content. In general, samples for micropaleontological analysis (benthic foraminifera) were taken at 10 (RD1 and RD3) and 15 cm intervals (core RD8) with a few additional samples at major transitions.

For granulometric analysis, a total of 42 samples were taken at 10 cm intervals from cores RD1 (11 samples), RD3 (14 samples), and RD8 (17 samples). Grain size measurements were carried out on 2 g of dry sediment, which underwent wet sieving using a 2000 µm mesh sieve to separate the coarse from the fine fraction (< 2000 µm). The fine fraction was then analyzed using a Malvern Mastersizer 3000 Laser Particle 139 Analyzer. One-half of each core is archived and stored at the GEOGLOB Laboratory at Sfax University (Tunisia).

Radiocarbon datings (^{14}C) were carried out at the Institute of Geology and Mineralogy at the University of Cologne, Germany. All samples were prepared following the standard procedure described in Délibrias (1985). Only intact mollusks, without sediment filling, were selected for dating. The shells were mechanically cleaned and leached with diluted HCl to remove portions of the shell matrix to prevent cross-reactions (Vita-Finzi and Roberts, 1984). Data calibration was performed by using MARINE 20 calibration curves (Heaton et al., 2020) and the CALIB radiocarbon calibration software (version 8.2), with a marine reservoir effect of 390 ± 85 years and $\Delta R = -104 \pm 109$ years (Hunt et al., 2020; Siani et al., 2000) for the Mediterranean Sea. The ages discussed below are expressed as median ages (cal BP and cal CE; Table 1).

For the identification of the gastropods and bivalves, we used the reference catalogues of Bouchet and Rocroi (2005, 2010). For micropaleontological analyses, core samples were dehydrated at 40 °C, and their dry weight was recorded. Samples were then washed over 63 µm mesh sieves and dried at room temperature. At least 300 specimens of benthic foraminifera were picked from each sample. Foraminifera were identified to species level and counted (Fig. 2, Table 2, Files S1–S3 in the Supplement) and then standardized to 2 g of dry sediment for each sample. Foraminifera records include all taxa. For the identification of species, we follow the taxonomic catalogues provided by Cimerman and Langer (1991) and Langer and Schmidt-Sinns (2006). The sample material is stored in the GEOGLOB laboratory of the University of Sfax, Tunisia (Mohamed Kamoun and Chahira Zaibi).

In order to reconstruct environmental changes along the coastline, benthic foraminifera were categorized according to their ecological (Table 3) and microhabitat preferences (Murray, 2006; Langer, 1988, 1989, 1993; Langer et al., 1998; Hayward et al., 1999, 2021).

Five groups were recognized: (I) ammoniid foraminifera as indicators for particularly shallow, intertidal, or stressed environmental conditions; (II) elphidiid foraminifera as indicators for shallow, nearshore coastline habitats; (III) miliolids as indicators for shallow coastline habitats; (IV) pen-

Figure 1. **(a)** Location map of the study area. **(b)** Map of the coastal area between Mahdia and Monastir showing Dzira Lagoon, capes, bays, and sabkhas. **(c)** Distribution of littoral environments (lagoon, island, coastal line), geomorphological units (swash bars, sand spit), and the direction of dominant longshore currents. **(d)** Morphologic changes in the tidal channel between 2006 and 2013 as recorded from satellite observations. **(e)** Location of the ancient city of Thapsus showing Roman harbors, breakwater moles of the piers, and sites of remaining ruins (Younes, 1999). **(f)** Area at the extremity NW of Dzira Island showing sand spits and swash bars (source Google Earth, mission 3-2013). **(g)** A 17th century copper engraving after Giocondo and Palladio (1567) showing a scheme of the Battle of Thapsus with the city of Thapsus and the Dzira Lagoon (lower right corner). For **(b)**, **(c)**, **(d)**, and **(f)**: © Google Earth.

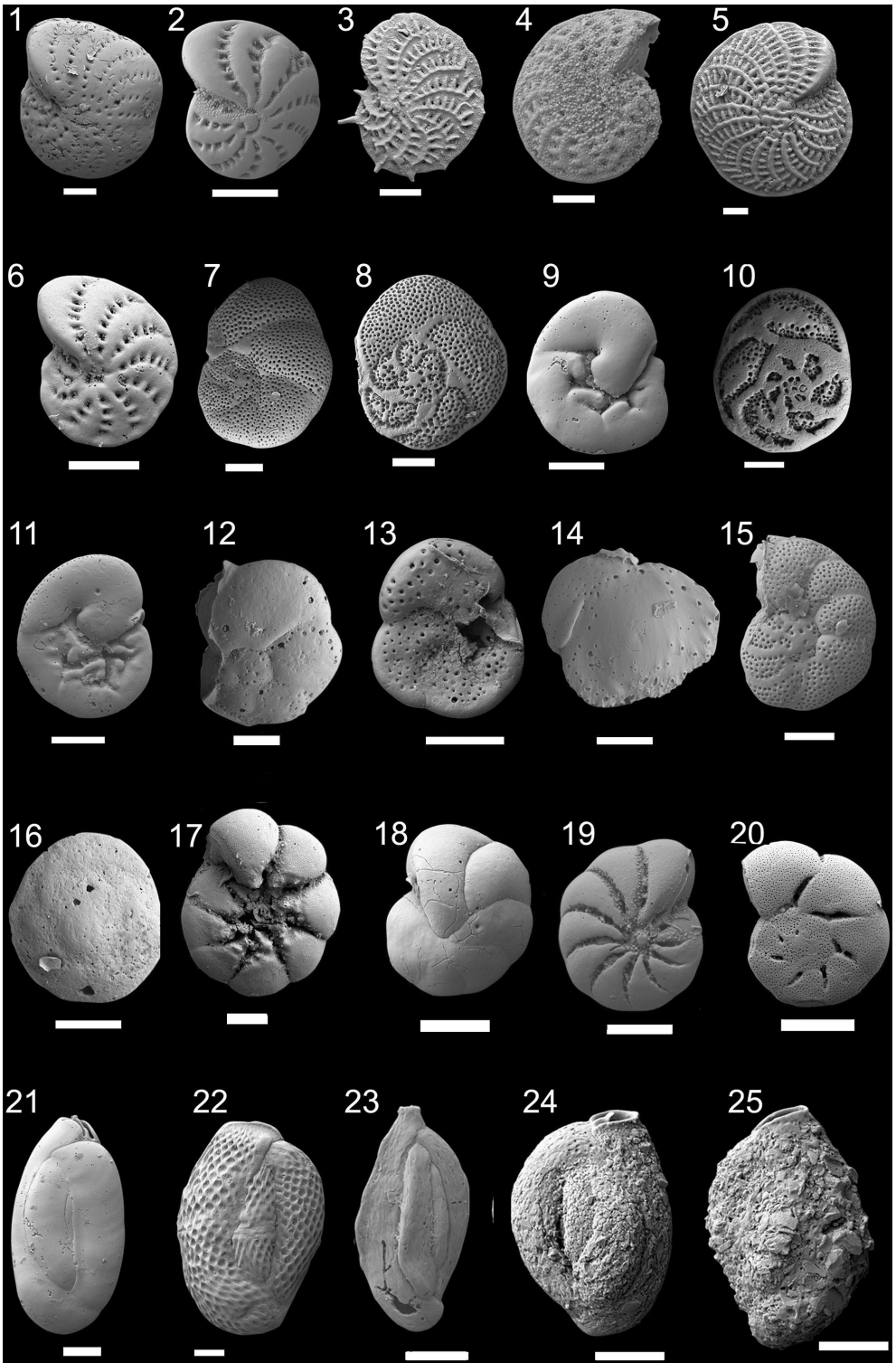

Figure 2. Scanning electron microscopy (SEM) photographs of foraminifera species found in sediments from cores RD1, RD3, and RD8. The scale bar is 100 µm for all specimens illustrated. **(1)** *Elphidium hawkesburiense* (Albani 1974). **(2)** *Elphidium advenum* (Cushman 1922). **(3)** *Elphidium aculeatum* (d'Orbigny 1846). **(4)** *Elphidium* sp. 1. **(5)** *Elphidium macellum* (Fichtel and Moll, 1798). **(6)** *Elphidium* cf. *E. limbatum* (Chapman, 1907). **(7–9)** *Rosalina bradyi* (Cushman 1915). **(10–11)** *Rosalina macropora* (Hofker, 1951). **(12–13)** *Rosalina* sp. 1. **(14)** *Siphonina tenuicarinata* Cushman, 1927. **(15)** *Discorbina* sp. 1. **(16)** *Neoconorbina* sp. 1. **(17)** *Ammonia venecpeyreae* Hayward and Holzmann, 2019. **(18)** *Discorbinella* sp. 1. **(19)** *Haynesina* sp. 1. **(20)** *Helenina anderseni* (Warren, 1957). **(21)** *Quinqueloculina tantabiddyensis* Parker, 2009. **(22)** *Lachlanella variolata* (d'Orbigny, 1826). **(23)** *Quinqueloculina* sp. 2. **(24)** *Siphonaperta dilatata* (Le Calvez & Le Calvez, 1958). **(25)** *Siphonaperta* sp. 1.

Table 1. ^{14}C ages obtained from bivalves and gastropods from cores RD1, RD3, and RD4.

Core	Coordinates	Total depth (cm)	Sampling depth (cm)	Studied material	Age ^{14}C yr BP	Range 1σ (68.3 %) cal yr BP	Range 2σ (95.4 %) cal yr BP	Median age cal yr BP	Median age BCE/CE	Laboratory code
RD1	35°37′37.80″ N 11°2′45.10″ E	90	76	*Cerithium vulgatum*	2472 ± 36	1713–1948	1743–2370	2079	129 BCE	COL6148.1.1
RD3	35°37′55.17″ N 11°2′38.17″ E	125	120	*Hydrobia trochulus* *Loripes lucinalis*	3147 ± 53	2747–3059	2604–3256	2913	963 BCE	COL4849.1.1
RD8	35°38′5.31″ N 11°2′28.98″ E	180	57–65	*Cerithium vulgatum* *Cerastoderma glaucum*	1779 ± 34	1138–1407	997–1545	1280	670 CE	COL6150.1.1
			108–116	*Cerithium vulgatum* *Cerastoderma glaucum*	2628 ± 36	2103–2437	2628–1953	2273	323 BCE	COL4852.1.1
			163–166	*Cerithium vulgatum* *Cerastoderma glaucum*	4076 ± 38	3893–4237	3729–4405	4070	2120 BCE	COL6151.1.1

eroplids as indicators for the presence of well-oxygenated seagrass or algal habitats; and (V) rosalinid foraminifera as indicators for algal or other hard-substrate environments. To compute and illustrate biocenotic parameters (abundance, number of individuals, species richness – NS, dominance – D, Shannon – H, and equitability – E indices; Pielou, 1966) the software package PAST V 2.04 (Hammer et al., 2001) was used (Files S1, S2, S3).

To determine the structure in the foraminiferal data, an R-mode cluster analysis was performed with the paired group algorithm using the Bray–Curtis dissimilarity for species constituting ≥ 2 % in at least one sample. Cluster analysis was performed on the foraminiferal sample data recorded in core RD3. Core RD3 was selected herein because it outperformed the other cores in microfauna richness. Cluster analysis is a large-scale analytical procedure to detect structural entities within complex data sets. This entails data mining and pattern discovery. For the cluster analysis, the data were imported into PAST software and analyzed. This technique groups together species with similar occurrence records in cluster assemblages and reveals a typology of environmental signatures embedded in a hierarchical dendrogram.

3 Core lithology and microfaunal record

3.1 Core RD1

Core RD1 has a total length of 90 cm, contains the highest foraminiferal species richness and abundance values, and is subdivided into three lithological units (Fig. 3, File S1, Table S1 in File S4).

Unit U1, from 90 to 70 cm, is composed of dark fine sands rich in organic matter. It contains mollusks, such as *Cerithium vulgatum, Hydrobia trochulus*, and *Loripes lucinalis*, as well as *Posidonia* seagrass debris and reveals the highest percentage of very fine sand (15 %), silt, and clay (10 %). The foraminiferal assemblages in this interval (70–80 cm, Figs. 4, 5) are characterized by moderate species richness and a mixture of nearshore (*Ammonia* spp.), shallow-water (miliolids), and typical epiphytic foraminifera (*Rosalina* spp., peneroplids). At a core depth of 75 cm (upper part of unit U1), an age of 2079 cal yr BP was obtained by ^{14}C radiocarbon dating.

Unit U2 (70 to 35 cm), mainly composed of medium and fine sand, contains various centimetric bands of gray sand that is rich in *Posidonia* debris and shows a peak of coarse quartz sand at a depth of 50 cm. Within the lower part of unit 2 (70–50 cm), foraminiferal species richness continues to rise and reaches its maximum at a core depth of 50 cm. The foraminiferal fauna in this interval is marked by nearshore (*Ammonia* spp.), shallow-coastal (*Elphidium* spp., miliolids), and abundant epiphytic taxa (*Rosalina* spp., peneroplids), indicative of an unrestricted connection of the tidal channel and/or navigation channel to the open sea. A peak of coarse sand recorded at 50 cm core depth is marked by a decrease

Table 2. Foraminifera taxa recorded in sediment samples from cores RD1, RD3, and RD8 in alphabetic order.

Acervulina mabaheti (Said, 1949)	*Quinqueloculina contorta* (d'Orbigny, 1846)
Ammonia convexa (Collins, 1958)	*Quinqueloculina limbata* (d'Orbigny, 1826)
Ammonia venecpeyreae Hayward & Holzmann, 2019	*Quinqueloculina seminulum* (Linnaeus, 1758)
Ammonia sp. 1	*Quinqueloculina ungeriana* d'Orbigny, 1846
Ammonia sp. 2	*Quinqueloculina vulgaris* d'Orbigny, 1826
Ammonia sp. 3	*Quinqueloculina* sp. 1
Asterigerinata mamilla (Williamson, 1848)	*Quinqueloculina* sp. 2
Bolivina sp. 1	*Quinqueloculina* sp. 3
Buccella granulata (di Napoli Alliata, 1952)	*Quinqueloculina* sp. 4
Bulimina sp. 1	*Quinqueloculina* sp. 5
Challengerella bradyi (Billman et al., 1980)	*Rosalina bradyi* (Cushman, 1915)
Cibicides refulgens (Montfort, 1808)	*Rosalina macropora* (Hofker, 1951)
Coscinospira hemperichii (Ehrenberg, 1839)	*Rosalina* sp. 1
Cycloforina sp. 1	*Rotorbis auberii* (d'Orbigny, 1839)
Cymbaloporella sp. 1	*Rotorboides granulosus* (Heron-Allen & Earland, 1915)
Discorbina sp. 1	*Sigmoilinita costata* (Schlumberger, 1893)
Elphidium aculeatum (d'Orbigny 1846)	*Cymbaloporetta* sp. 1
Elphidium advenum (Cushman 1922)	*Siphonaperta agglutinans* (d'Orbigny, 1826)
Elphidium crispum (Linnaeus, 1758)	*Siphonaperta dilatata* (Le Calvez & Le Calvez, 1958)
Elphidium fichtellianum (d'Orbigny, 1846)	*Siphonaperta* sp. 1
Elphidium hawkesburiense (Albani, 1974)	*Siphonina tenuicarinata* Cushman, 1927
Elphidium jenseni (Cushman, 1924)	*Sorites orbiculus* (Forskål, 1775)
Elphidium limbatum (Chapman, 1907)	*Spiroloculina angulata* (Cushman, 1917)
Elphidium macellum (Fichtel et Moll, 1798)	*Spiroloculina antillarum* (d'Orbigny, 1839)
Elphidium sagrum (d'Orbigny, 1839)	*Spiroloculina communis* Cushman & Todd, 1944
Elphidium williamsoni (Haynes, 1973)	*Spiroloculina regularis* (Cushman & Todd, 1944)
Elphidium sp. 1	*Spiroloculina* sp. 1
Elphidium sp. 2	*Triloculina* sp. 1
Haynesina depressula (Ehrenberg, 1840)	*Triloculina trigonula* (Lamarck, 1804)
Lachlanella variolata (d'Orbigny, 1826)	*Vertebralina striata* d'Orbigny, 1826
Nubecularia lucifuga (Defrance, 1825)	
Peneroplis planatus (Fichtel et Moll, 1798)	
Pseudotriloculina laevigata (d'Orbigny, 1826)	

in species richness and in the composition of foraminiferal biota. At 40 cm depth, species richness drops rapidly and reaches its lowest value, while *Ammonia* spp. constitutes more than 40 % of the benthic fauna. Peak abundances of *Ammonia* spp. and particularly low species richness values suggest a tendency towards more restricted conditions and are indicative of environmental changes that were initiated after the deposition of coarse sands.

Unit U3, from 35 cm to the sediment surface, is characterized by a mixture of fine (25 %) and medium sand (60 %) and lacks very fine sand, silt, and clay. From 30 to 10 cm core depth, foraminiferal species richness rises above 30 but drops to around 20 at 5 cm depth. At the same time, percent abundances of *Ammonia* spp. increase towards the core top, while the total number of individuals decreases continuously and reaches minimum values just below the sediment surface. Both the decrease in species richness and individual numbers and the increase in ammoniid foraminifera suggest that the connection with the open ocean continued to deteriorate.

3.2 Core RD3

Core RD3 has a total length of 130 cm and exhibits four different lithological units (Fig. 3, File S2, Table S2 in File S4). Unit Ul1 comprises the interval from 130 to 110 cm and mainly consists of dark, medium, and fine sands that are rich in mollusks (*Cerithium vulgatum, Hydrobia trochulus*, *Loripes lucinalis*) and *Posidonia* seagrass debris. At a core depth of 120 cm, radiocarbon dating revealed an age of 2913 cal yr BP for unit Ul1. Along the entire RD3 core, the silt and clay fractions are highest in unit Ul1. Species richness in Ul1 ranges between 20 and 30, a range that remains almost constant throughout the core (Figs. 6, 7). The foraminiferal fauna in unit Ul1 is dominated by *Ammonia* spp. and *Rosalina* spp. but also contains various species of *Elphidium* and miliolid foraminifera. The diverse composition suggests a shallow nearshore setting with free connections to the open sea.

Unit Ul2 (110–90 cm) is composed of gray sands that are rich in mollusks. Above Ul2, white sands were deposited and

Table 3. Environmental preferences of dominant species and genera of benthic foraminifera recorded along cores RD1, RD3, and RD8.

Genus/species	Environmental preferences	References
Ammonia convexa	Restricted to intertidal environments. Preference for mud and muddy sand substrates and tolerates a wide range of normal marine to hyposaline salinities. Stress-tolerant and used here as an indicator for the closure of the lagoon.	Saad and Wade (2016), Bird et al. (2020), Hayward et al. (2021), Blanc-Vernet et al. (1979)
Asterigerinata mamilla	Associated with shallow phytal substrates or sandy bottoms in well-oxygenated environments.	Langer (1988, 1993), Frezza and Carboni (2009)
Buccella granulata	Indicator species for shallow-water habitats (0–100 m) characterized by fine sands and mud. Mostly infaunal and rarely as epiphyte.	Avnaim-Katav et al. (2015), Blanc-Vernet et al. (1979), Morigi et al. (2005), Murray (2006), Calvo-Marcilese and Langer (2012)
Cibicides refulgens	Epiphyte on various types of algae and seagrasses with a preference for shallow coastal, nearshore habitats. Also present on hard substrates such as mollusk shells and pebbles.	Langer (1988, 1993), Oflaz (2006)
Discorbinella	Indicator taxon for infralittoral to circalittoral shallow nearshore environments including tidal channels. Occurs together with other oxic species such as *Cibicides*, *Planorbulina*, and smaller miliolids	Kaminski et al. (2002), Oflaz (2006), Armynot du Châtelet et al. (2018)
Elphidium crispum, *Elphidium fichtellianum*, *Elphidium jenseni*, *Elphidium macellum*, *Elphidium sagrum*	Most elphidiid foraminifera are indicators for shallow, nearshore environments that are well-connected to the open ocean. Often epiphytic on phytal substrates and within rhizomes of *Posidonia*. Some species have microhabitat preferences for sandy and muddy substrates and occur over a wide range of habitats (brackish–hypersaline marshes and lagoons, inner shelf settings).	Murray (2006), Langer (1988, 1993), Langer et al. (1990, 1998)
Haynesina depressula	Mostly infaunal in muddy and silty shallow-water environments. Occurs over a range of habitats from brackish, intertidal to lagoon environments and tolerates a wide range of salinity and temperature conditions.	Calvo-Marcilese and Langer (2010), Langer et al. (1990), Murray (2006)
Laevipeneroplis karreri, *Peneroplis planatus*, *Peneroplis pertusus*	Larger symbiont-bearing foraminifera with preferences for various types of phytal substrates in shallow-water settings. Living species in the Mediterranean Sea are mostly restricted to depth between 0 and 50 m.	Cimerman and Langer (1991), Langer (1988, 1993), Murray (2006)
Siphonaperta agglutinans	Occurs frequently in rhizome habitats of the seagrass *Posidonia oceanica.*	Langer (1988, 1993), Langer et al. (1998)
Neoconorbina	Epiphytic, common in Mediterranean infralittoral environments, typical taxa in well-oxygenated, shallow-marine environments covered by algae or seagrasses. Also present in inner shelf environments and on hard substrates.	Cimerman and Langer (1991), Dimiza et al. (2016), Frezza and Carboni (2009), Langer (1988, 1993), Murray (2006)
Quinqueloculina seminulum, *Quinqueloculina vulgaris*, *Triloculina trigonula*	Miliolids occur over a wide range of shallow-water habitats, often observed on phytal substrates but also shallow infaunal. Preferences for well-oxygenated shallow and open-shelf settings covered by algae and seagrasses.	Langer (1988, 1993), Murray (2006), Sgarrella and Moncharmont Zei (1993)
Rosalina bradyi, *Rosalina macropora*	Mostly epiphytic in Mediterranean shallow-water environments. Present on algae, seagrasses, and rhizomes in well-oxygenated habitats.	Langer (1993), Frezza and Carboni (2009), Langer et al. (2013)

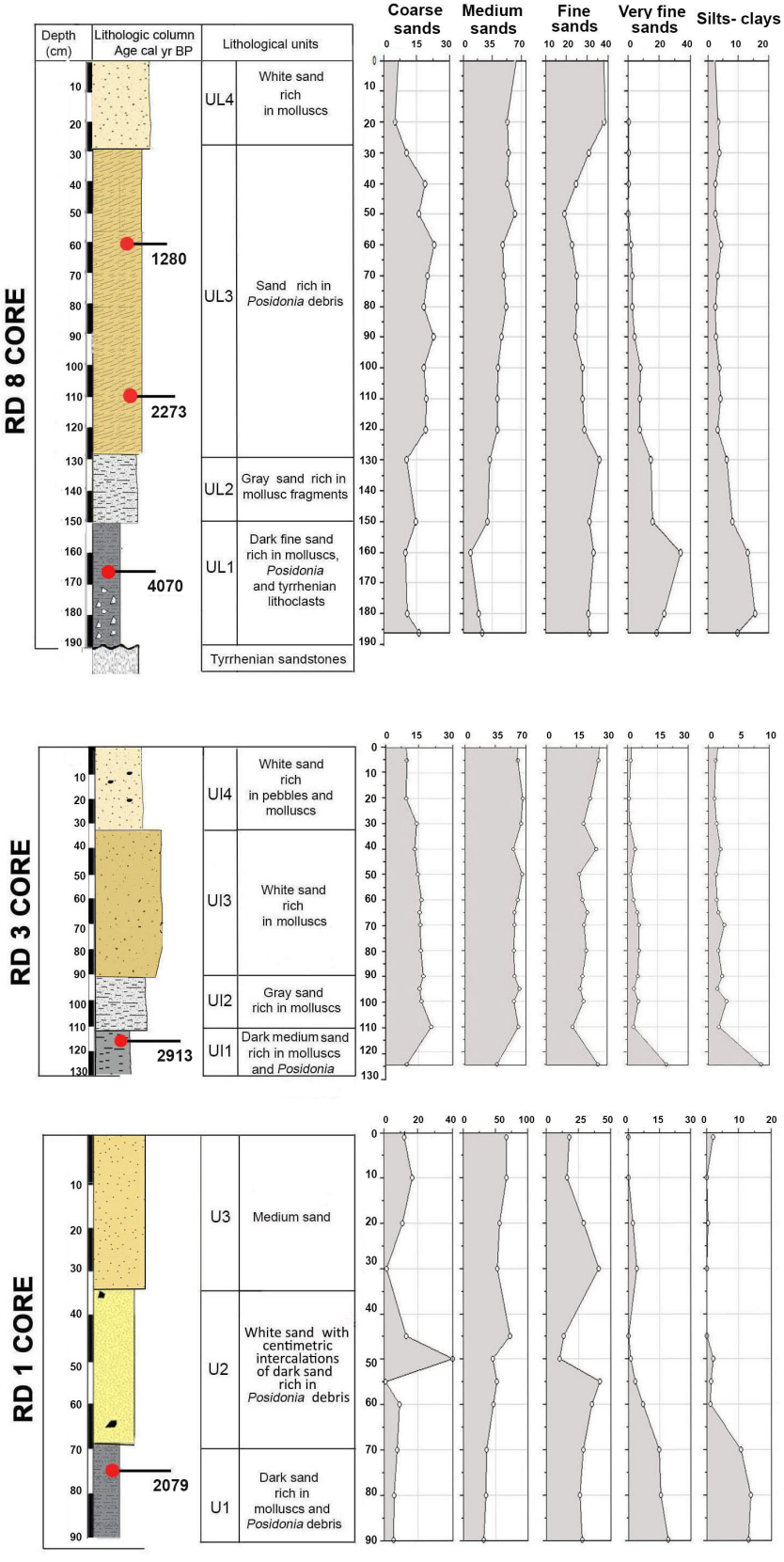

Figure 3. Lithologic columns and lithological units, calibrated median ages (yr BP), and textural components (percentages of grain size classes: coarse sand, medium sand, fine sand, very fine sand, and silt–clay) for cores RD1, RD3, and RD8.

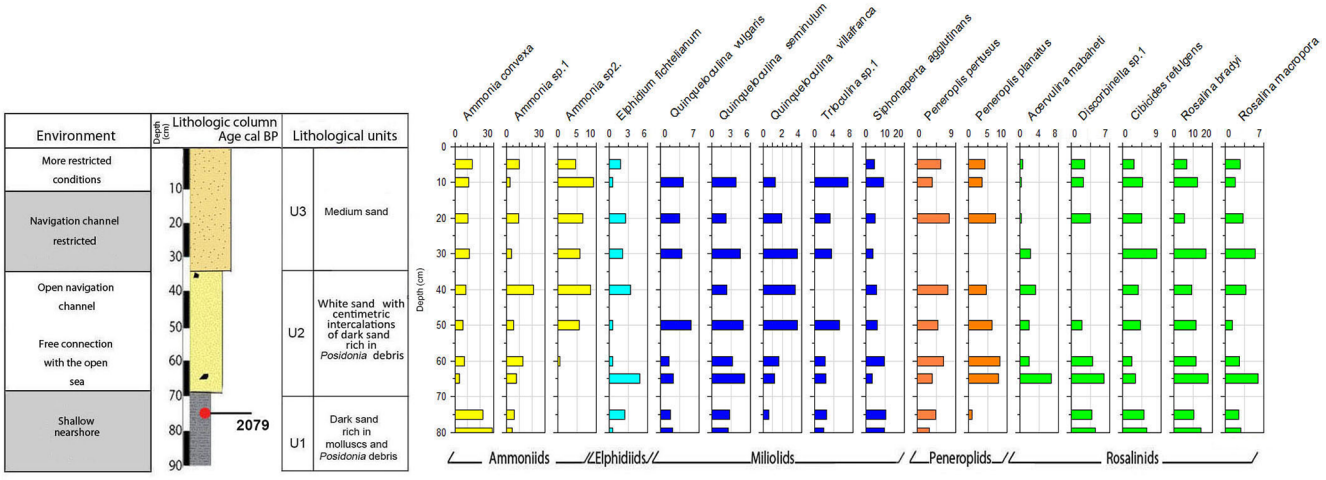

Figure 4. Foraminifera data for core RD1: depth of core, calibrated median ages (yr BP), lithological units, vertical distribution of foraminifera, and environments.

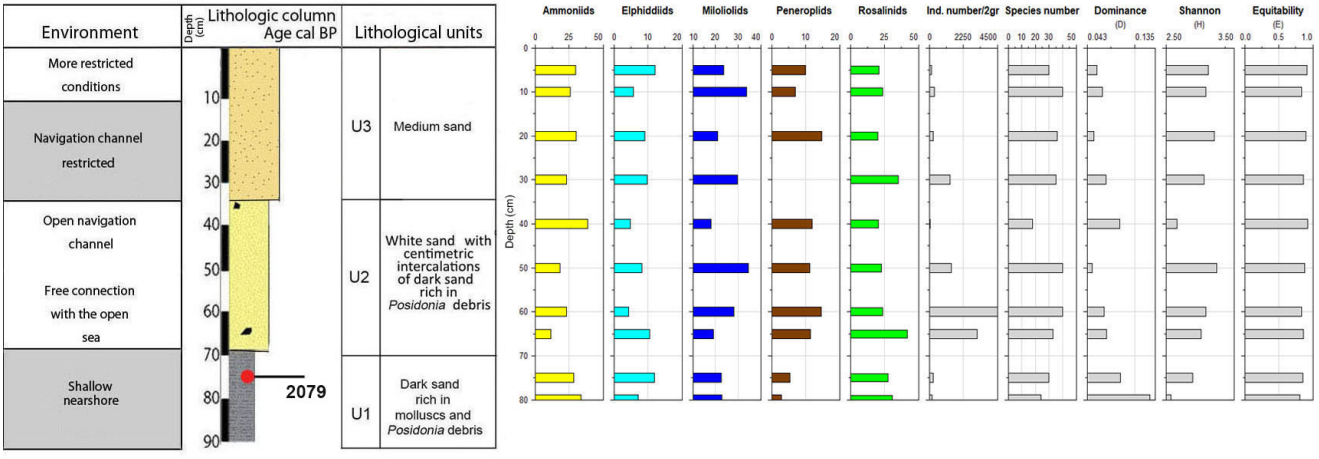

Figure 5. Foraminifera data for core RD1: depth of core, calibrated median ages (yr BP), lithological units, vertical distribution of foraminiferal groups, biocenotic parameters, diversity indices, and environments.

constitute unit Ul3. Unit Ul3 extends from 90–35 cm core depth and contains abundant intact and fragmented shells of *Cerithium vulgatum* and *Dentalium* sp. Towards the top of this unit, the percentage of medium and fine sand gradually increases and reaches values of 65 % and 20 %, respectively. Species richness within units Ul2 and Ul3 ranges between 20 and 30, but the number of individuals decreases continuously towards the top of the core. The faunal assemblages recorded in Ul2 and Ul3 are heterogenous, reveal percent abundance variations between coastal water indicators (*Ammonia* spp.), elphidiids, and *Rosalina* spp., and display peak abundances of epiphytic peneroplids and smaller miliolids between 70 and 40 cm core depth. Peak abundances of peneroplid and miliolid foraminifera coincide with lowest values of ammoniid foraminifera and suggest a free connection to the open sea. However, abundance variations of peneroplid–miliolid and ammoniid foraminifera suggest that the free connection to the open ocean varied over time.

The top portion of the core (35–0 cm) represents unit Ul4 and comprises white sands that contain abundant pebbles and mollusks (*Loripes lucinalis*, *Abra alba*, *Cerithium vulgatum*, *Potamides* sp., *Natica* sp.). Within unit Ul4, coarse sands gradually decrease and the deposits are dominated by medium (70 %) and fine (20 %) sands. The foraminiferal fauna of unit Ul4 is marked by low species richness and abundance values, low percent abundances of smaller miliolids, and continuously rising rates of coastal indicator foraminifera (*Ammonia* spp.). The faunal shift recorded in unit Ul4 suggests a tendency towards more restricted con-

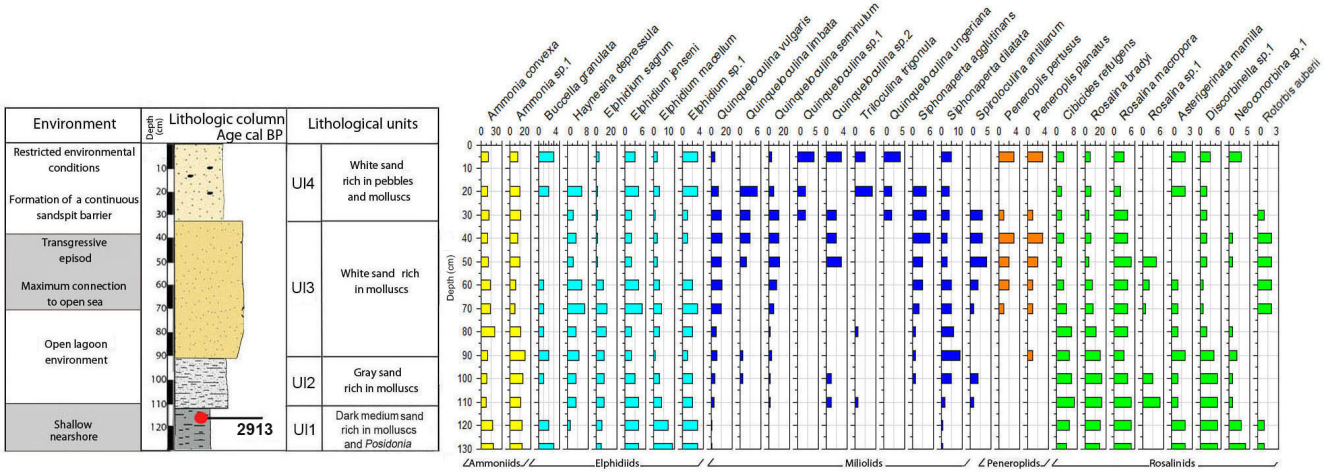

Figure 6. Foraminifera data for core RD3: depth of core, calibrated median ages (yr BP), lithological units, vertical distribution of foraminifera, and environments.

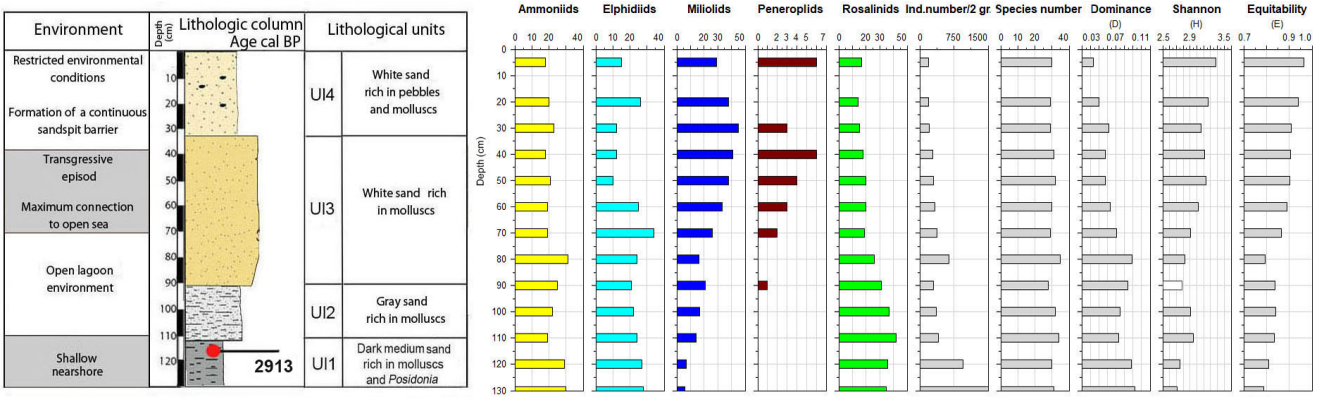

Figure 7. Foraminifera data for core RD3: depth of core, calibrated median ages (yr BP), lithological units, vertical distribution of foraminiferal groups, biocenotic parameters, diversity indices, and environments.

ditions with a limited exchange of coastal waters with the open-ocean environment.

3.3 Core RD8

Core RD8 has a total length of 190 cm; unlike RD1 and RD3 and due to its length, it reached the white upper Pleistocene carbonate sandstones at its base (Fig. 3). The sediments deposited above the Pleistocene sandstones exhibit four different lithological units (UL1–UL4). Unit UL1, from 190 to 150 cm, is composed of dark fine sands that are rich in mollusk fragments, *Posidonia* seagrass debris, and Tyrrhenian lithoclasts. Mollusk shells collected at a core depth between 163 and 166 cm were dated and revealed an age of 4070 cal yr BP. Unit UL1 is rich in silt–clay (15 %) and very fine sand (20 %), a pattern that continues throughout the rest of the core. The foraminiferal biota (Figs. 8, 9; File S3, Table S3 in File S4) of unit UL1 contain abundant individuals of the coastal shallow-water genus *Ammonia*, largely absent in this unit. Both the number of species and the number of individuals per gram dry sediment are comparatively high, indicative of a shallow, well-oxygenated habitat that is connected to the open ocean.

Gray sands constitute unit UL2 (150 to 130 cm) and show a decrease in the silt–clay and very fine sand fraction as well as an increase in medium sands (35 %). Unit UL2 hosts diverse, species-rich, and heterogenous assemblages of foraminifera, indicative of a continuation of a free connection to the open sea.

Unit UL3 (130 to 30 cm) differs from other units by the enrichment of coarse sand (20 %) and *Posidonia* seagrass debris. Mollusk shells used for radiocarbon dating revealed an age of 2273 and 1280 cal yr BP for sediments deposited at 108–116 and 57–65 cm core depth, respectively. Unit UL3 is characterized by an increase in medium (40 %) and coarse sands (20 %). Within the lower portion of this unit (120–70 cm core depth), epiphytic peneroplids are strikingly more

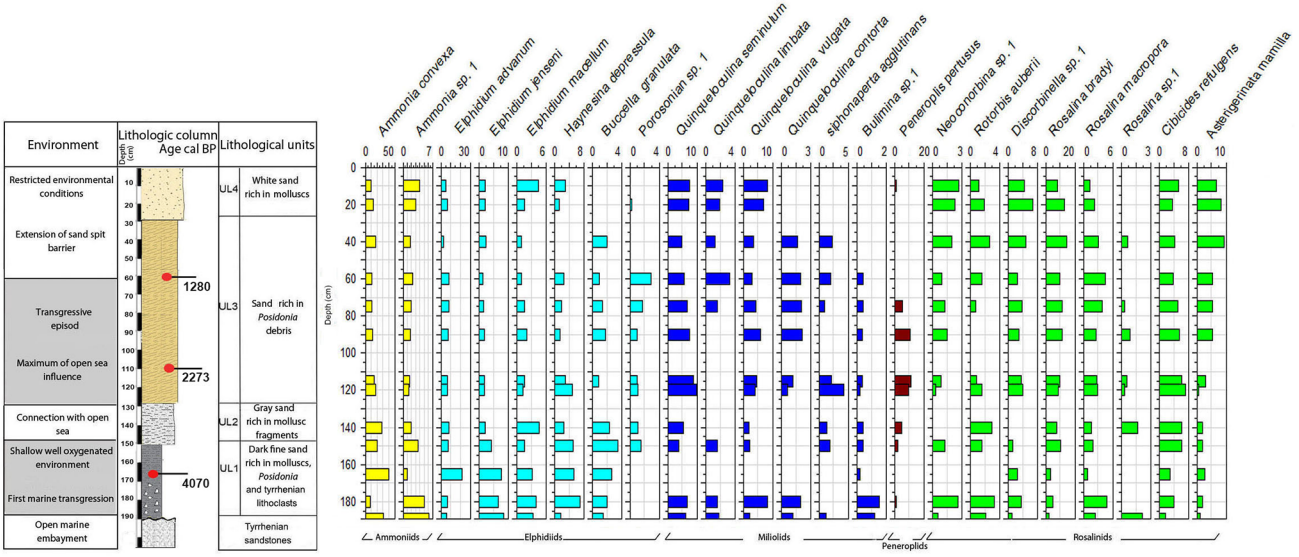

Figure 8. Foraminifera data for core RD8: depth of core, calibrated median ages (yr BP), lithological units, vertical distribution of foraminifera, and environments.

abundant and contribute ∼ 10 % to the total assemblage. At the same time, the abundance of shallow coastal water indicators (*Ammonia* spp.) decreases. Above 65 cm core depth, peneroplid foraminifera disappear almost completely, the number of ammoniid foraminifera increases, and the species richness and the number of individuals per gram sediment continue to decrease. The observed shift from high- to low-diversity assemblages, the lack of epiphytic peneroplids, and the increase in specimens of *Ammonia* spp. suggest a transition from open-ocean to more restricted environmental conditions.

White sands rich in mollusk shell debris constitute unit UL4 (30 cm to core top). This unit is characterized by a prominent decrease in coarse sands and an enrichment of the fine sand fraction (40 %). The foraminiferal fauna recovered from unit UL4 is marked by low species richness values, a lack of peneroplids, abundant specimens of *Rosalina* spp., *Ammonia* spp., *Elphidium* spp., and low numbers of individuals per gram dry sediment. All parameters show an increasing constriction of the lagoon and a worse connection with the open ocean.

4 Cluster analyses of foraminifera taxa

Cluster analysis was performed to obtain additional paleoenvironmental information (Figs. 10, 11) and included all taxa from core RD3 constituting at least 2 % in one sample. The 2 % limit was selected to reduce background noise from rare species and resulted in a total of 39 taxa to be included. The total number of species recorded in core RD3 was 50. Results of the R-mode analysis revealed the presence of six clusters (CL1 to CL5, Fig. 10a). Cumulative percentage data for all species contributing to individual clusters are provided across the RD3 core (Fig. 10b).

Cluster 1 (CL1) occurs continuously throughout the core and shows peak species richness values between 50 and 20 cm. It contains *Ammonia* sp. 2 (3 %), *Ammonia* sp. 3, *Peneroplis pertusus* (3 %), *Peneroplis planatus* (3 %), *Elphidium crispum* (2 %), *Coscinospira hemprichii* and various robust miliolids (*Lachlanella variolata* (3 %), *Quinqueloculina* sp. 1, *Quinqueloculina* sp. 2, *Quinqueloculina ungeriana* (3 %), and *Triloculina trigonula* (5 %). The species recorded are indicative of a particularly shallow, current-dominated environment characterized by coarse-grained sediments (García-Sanz et al., 2018; Buosi et al., 2012).

Cluster 2 (CL2) is represented by *Quinqueloculina limbata* (5 %), *Siphonaperta agglutinans* (5 %), *Rotorbis auberii* (2.5 %), and *Spiroloculina antillarum* (3 %). It shows the highest percentages (10 %–17 %) in the interval between 60 and 20 cm and is indicative of an open lagoon environment and a free connection to the sea.

Subcluster 3A (CL3A) contains abundant elphidiids, *Cibicides refulgens* (7 %), *Elphidium jenseni*, *Discorbinella* sp. 1, *Elphidium macellum* (9 %), *Elphidium* sp. 1, *Haynesina depressula* (6 %), *Siphonaperta dilatata* (9 %), and *Rosalina macropora* (5 %). *Haynesina depressula* has frequently been reported from muddy sands of intertidal environments (Langer, 1988). These taxa occur continuously throughout the core. Maximum abundances were recorded in the lower part of the core (130–60 cm, 37 %).

Subcluster 3B (CL3B) contains *Quinqueloculina vulgaris* (10 %), *Quinqueloculina seminulum* (10 %), *Ammonia* sp. 1 (15 %), *Rosalina bradyi* (15 %), *Ammonia aberdoveyensis* (20 %), and *Elphidium sagrum* (10 %). CL3B shows the max-

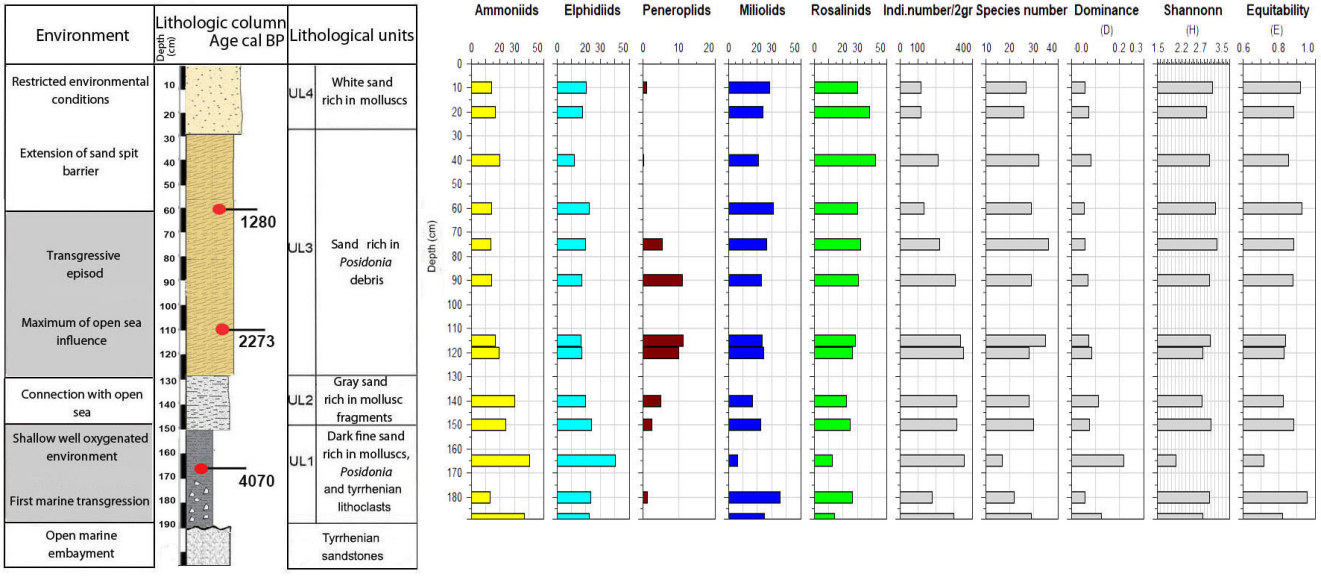

Figure 9. Foraminifera data for core RD8: depth of core, calibrated median ages in BP, lithological units, vertical distribution of foraminiferal groups, biocenotic parameters, diversity indices, and environments.

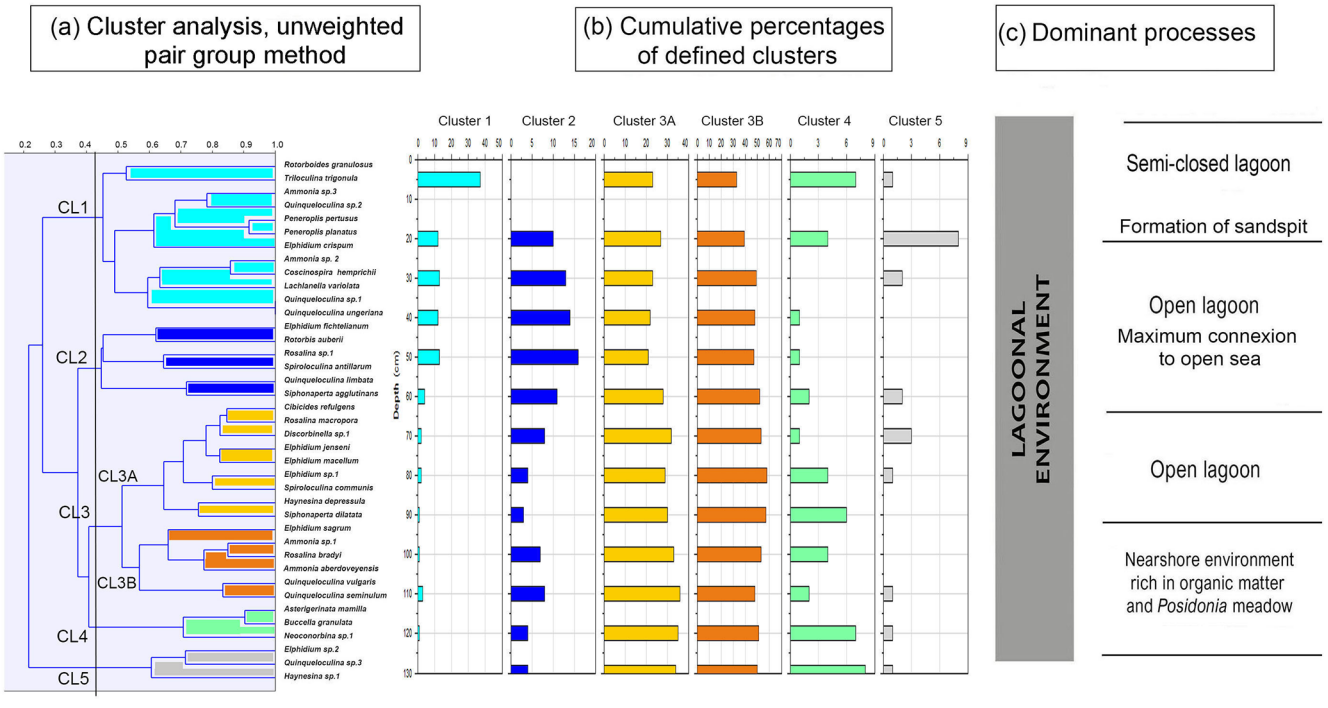

Figure 10. R-mode cluster analysis for core RD3 showing clusters CL1 to CL5.

imum richness (50 %) between 110 and 60 cm. To the top of the core the richness is around 37 %. Subclusters 3A and 3B are interpreted to represent nearshore environments.

Cluster 4 (CL4) occurs continuously throughout the core. It contains motile epiphytic species (*Buccella granulata*) and a range of temporarily attached forms (*Asterigerinata*, *Neoconorbina*). It shows sporadic occurrences (6 %) in its basal part between 130 and 80 cm. Cumulative percentage data decrease markedly between 70 and 30 cm. Taxa of cluster CL4 are indicative of phytal substrates and sandy sediments (Frezza and Carboni, 2009; Blanc-Vernet et al., 1979; Langer, 1993).

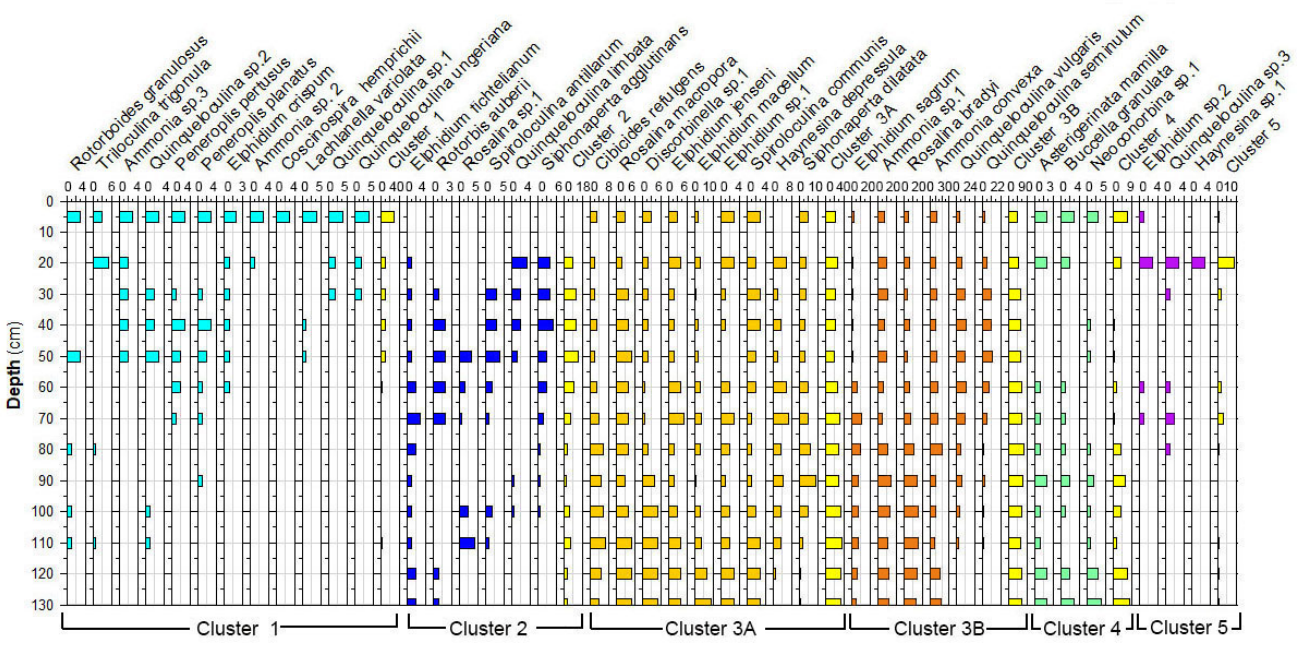

Figure 11. Relative abundances of all major species along core RD3.

Cluster 5 (CL5) is discontinuously present along the core and includes *Quinqueloculina* sp. 3 (between 50 and 30 cm, 3 %), *Elphidium* sp. 2 (3 %), and *Haynesina* sp. 1 (3 %). Percentage data across the core show a range between 1.5 and 3 % for species of this cluster with a maximum between 80 and 60 cm core depth. *Elphidium* sp. 2 occurs widely from infralittoral to circalittoral environments but also on leaves of phytal substrates (Sgarrella and Moncharmont Zei, 1993; Langer, 1993).

5 Discussion

The analyses of both sedimentological and micropaleontological multi-proxy data from core material collected off the coast of Thapsus allow (i) reconstruction of a scenario for the paleoenvironmental and morphodynamic evolution for the past ∼ 4000 years (Fig. 12), (ii) an assessment of the impact of natural and anthropogenic factors, and (iii) a comparison to models developed for coastal wetlands, floodplains, and lake environments from Tunisia and other Mediterranean coastal environments.

The base of core RD8 revealed carbonate sandstones (Fig. 13a) that are upper Pleistocene in age (marine isotopic substage 5e, Jedoui et al., 1998). They are commonly referred to the Tyrrhenian facies (Paskoff and Sanlaville, 1983) and can be correlated with carbonate sandstones outcropping along the northern coast of Sfax (Khadraoui et al., 2019; Kamoun et al., 2020) and Djerba Island (Jedoui et al., 1998). Following a glacial sea level lowstand, coastal environments along Tunisia remained emerged. Marine deposits indicating flooding were then recorded along the southern Skhira coast and at the Hachichina wetlands dated to ∼ 7460 and ∼ 7890 cal yr BP, respectively (Zaibi et al., 2016; Ben Khalifa et al., 2019). The lack of such deposits in the RD1, RD3, and RD8 core material suggests that the Thapsus area remained emerged even longer as a result of neotectonic activity (from the upper Pleistocene to the Northgrippian, Figs. 12, 13b). In fact, the Thapsus coast belongs to the Sahel area characterized by major faults oriented in the NS, EW, NE–SW, and NW–SE direction. Recent tectonic events have reactivated these structures, resulting in a system of active faults such as the Skanes–Monastir fault. Neotectonic activity resulted in extensive faulting, driven by a compressive regime which continued from the Miocene to Quaternary (Bahrouni et al., 2014).

Evidence for a delayed marine transgression at Thapsus is also provided by the occurrence of marine sediments and biota. These sediments were deposited directly above the erosional contact on the white carbonate sandstones (Figs. 12, 13c) and indicate a rising sea level. The sediments are herein dated to 4070 cal yr BP (RD8 core, UL1, 165 cm depth) and are composed of fine sands that are rich in mollusk fragments, *Posidonia* seagrass debris, Tyrrhenian lithoclasts, and benthic foraminifera, indicative of an open marine, shallow nearshore habitat characterized by epiphytic forms that dwell on phytal substrates. High-energy conditions are also indicated by the dominance of gravelly, lithogenous, and clastic materials and by coarse (10 %), medium (20 %), and fine sand (30 %) sediments of unit UL1 (core RD8).

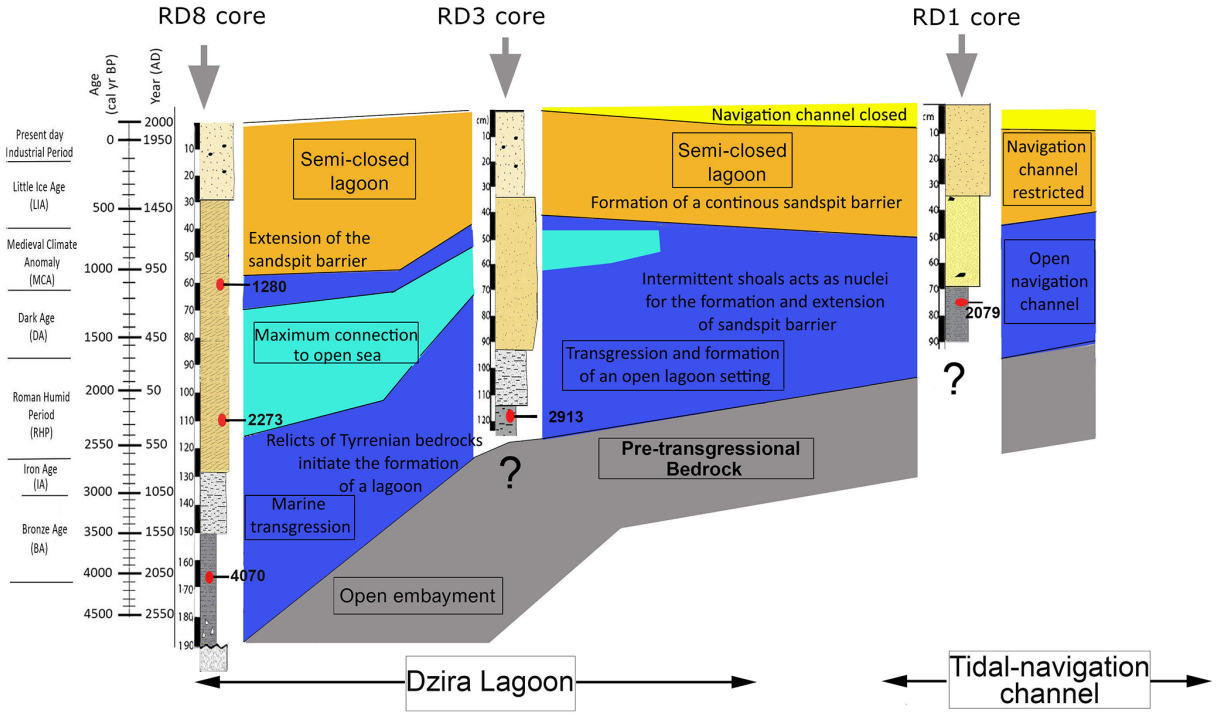

Figure 12. Diagrammatic illustration showing the stratigraphy of Thapsus subsurface sediments and dominant processes as inferred from micropaleontological and sedimentological proxies.

According to Jedoui et al. (1998), Morhange and Pirazzoli (2005), and Paskoff and Sanlaville (1983), the Holocene marine transgression peaked at around 3550–4050 cal BCE in southeastern Tunisia and in other parts of the Mediterranean (Kayan, 1999; Kraft et al., 2007). The transgressive sediments can be correlated with dated deposits from the northern Sfax coast (4500 cal yr BP; Khadraoui et al., 2018) and with material recorded from cores from the Gulf of Gabes, where the maximum sea level influence was recorded at around 4630 ± 160 yr BP (Morzadec-Kerfourn, 2002).

5.1 Origin of the Dzira Lagoon between 4070 and 2273 cal yr BP

A transition from an open nearshore setting towards a lagoonal environment is indicated by the microfauna recovered from sediments deposited in the lower part of unit Ul3 in core RD3. The foraminiferal assemblages in this zone are characterized by a distinct increase in *Ammonia aberdoveyensis* (28 %), the disappearance of typical marine taxa such as *Quinqueloculina ungerina*, *Rotorbis auberii*, *Spiroloculina antillarum*, and *Peneroplis planatus*, and a general increase in total abundances (300 individuals per 1 g). The reduction of marine taxa, the high percent abundances of *Ammonia* spp., and the rise of total abundances suggest more restricted and possibly lagoonal conditions in which nutrients accumulate (Carbonel, 1982). The formation of a lagoonal setting is also marked in core RD8 (between units UL1 and UL2), where total abundances and the number of stress-tolerant ammoniid taxa increase, while shallow-water miliolids and epiphytes decrease. The transition from an open marine setting (∼ 4070) towards a lagoonal environment (until 2273 cal yr BP) was probably favored by the presence of discontinuous shoals (Oueslati, 1993) and the action of littoral drift currents, allowing the genesis of a long sand spit (Fig. 13d). Similar conditions were recorded in unit U1 of core RD1 (dated at 2079 yr BP), where brackish, shallow-water taxa prevail together with other marine taxa. However, the mixture of brackish water (*Ammonia*) and marine taxa suggests that the communication of the Dzira Lagoon with the open sea, although now limited, continued to exist. This finding is supported by archeological data from Younes (1999), who reported increased silting during this time interval and noted that only small boats were able to access the Roman harbor Portus Pristinus via a tidal channel into the Dzira Lagoon. The formation of approximately time-equivalent sand spits along the coast of Tunisia was also reported by Khadraoui et al. (2018) from the northern Sfax coast, from Bin El Oudiane at Djerba Island (Masmoudi et al., 2005), from the Hachichina wetlands (Ben Khalifa et al., 2019), and from Rass Boutria at Acholla (Kamoun et al., 2019, 2020). A progradation of coastal and lagoonal environments was also reported from Boujmel by Lakhdar et al. (2006).

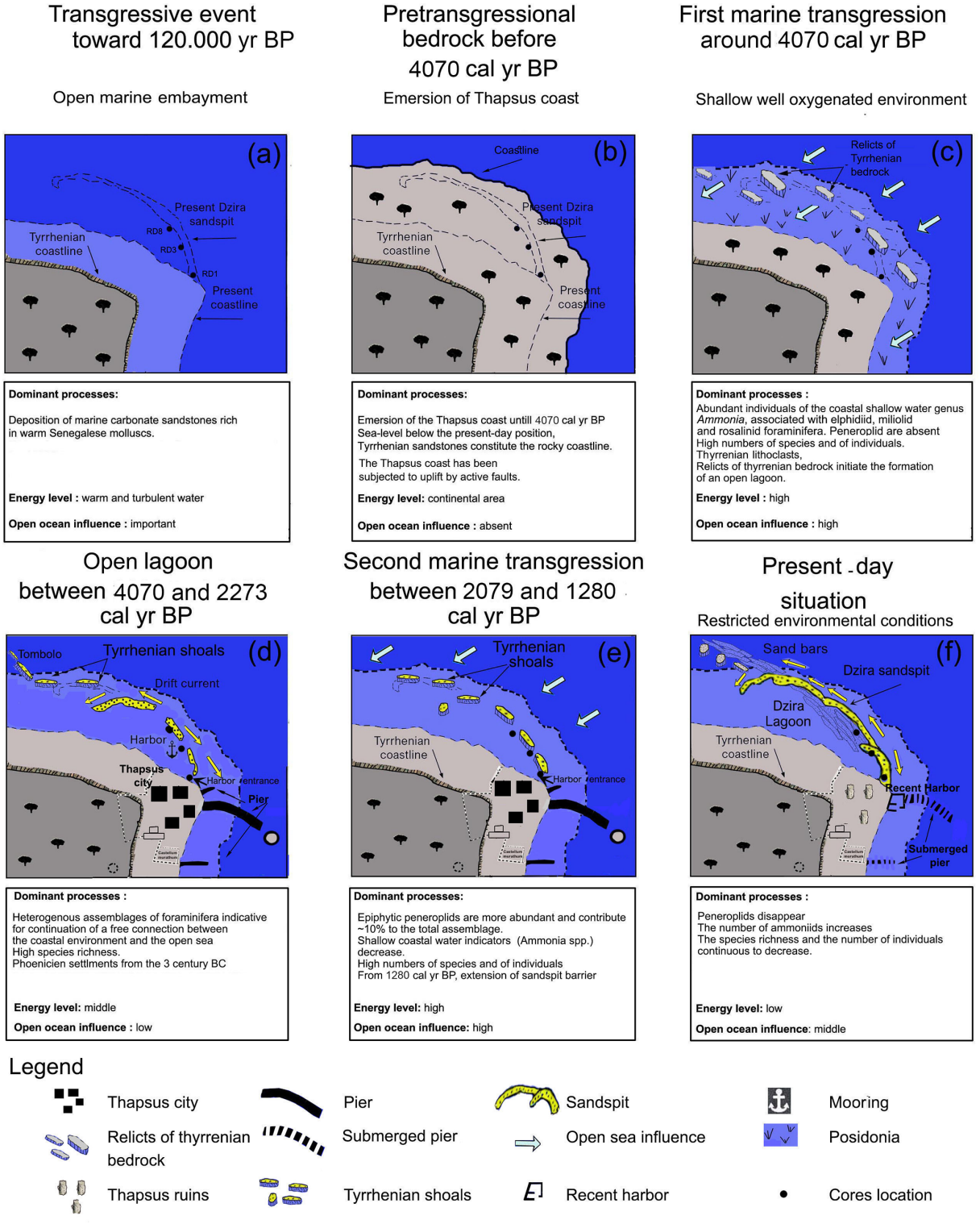

Figure 13. Environmental evolution of the Thapsus coast and the Dzira Lagoon as inferred from micropaleontological and sedimentological core data. For each stage the dominant processes, the efficiency of the energy level and the oceanic and anthropogenic influence on the development of the lagoon are documented.

5.2 The second marine transgression between 2079 and 1280 cal yr BP

A second marine transgression between 2079 and 1280 cal yr BP is indicated by faunal assemblages recorded in the upper part of unit Ul3 in core RD3. This transgression is characterized by the dominance of smaller miliolid foraminifera, the presence of symbiont-bearing peneroplids (*Laevipeneroplis karreri*, *Peneroplis planatus*), and the highest species richness values recorded across the core (50 species). These assemblages are commonly associated with seagrass meadows (leaves and rhizome microhabitats) and other phytal substrates (algal thalli) (Langer, 1993; Langer et al., 2013; Mateu-Vicens et al., 2010). Sediments within this unit show an increase in medium sand and a reduction of very fine sand, clay, and silt. Both the foraminiferal biota and the grain size recorded suggest that the semi-enclosed lagoonal habitat re-established connections with the open sea (passages) to form an open lagoon environment between 2079 and 1280 cal yr BP (Fig. 13e). Findings of time-equivalent transgressions from the nearby northern (1396 yr cal BP; Khadraoui et al., 2018) and southern Sfax coast (1900 cal yr BP; Gargouri et al., 2007) support the hypothesis of a second transgression during this time interval. In addition, archeological studies conducted by Anzidei et al. (2011) on Punic and Roman materials from along the coast of Tunisia showed that the local relative sea level increased by 0.2 to 0.5 m over the last 2 kyr.

5.3 The formation of a semi-closed lagoon from 1280 cal yr BP

Depositional regime changes are again indicated by sediments deposited after 1280 cal yr BP. Foraminiferal faunal analysis of these deposits (unit Ul4 in core RD3, in the upper part of UL3, and in UL4 of core RD8) show that both the species richness and the number of individuals decrease. In addition, the number of stress-tolerant ammoniid foraminifera increases, while miliolid taxa decrease. Reduced species richness values, rising numbers of stress-tolerant taxa, and decreasing H and E indices suggest a deterioration of environmental conditions, possibly indicating a transition to semi-enclosed lagoonal conditions. At the top of core RD3 and RD8, medium and fine sand fractions increase substantially (90 %) and mark the increasing closure of the lagoonal environment. Driving forces of the environmental transformation include a steady accretion of sand deposits favored by longshore sediment drift, ultimately resulting in an elongation of the offshore sand spit.

Within unit U2 of core RD1, which is the core located just next to the present-day and presumably old entrance channel, the foraminiferal fauna displays a substantial rise of stress-tolerant indicator taxa (*Ammonia* spp. 30 %), indicative of more restricted environmental conditions. Indeed, archeological studies showed that the lagoonal environment during this time interval was used as a harbor, where silting of the entrance channel necessitated human interventions to keep the entrance channel open to the sea (Carayon, 2008). Potential indications for dredging include abrupt fluctuations in both the number of individuals per gram sediment and in the number of species across this interval (50 and 4600 individuals per 2 g sediment, 18 to 38 species). Because core data from neither RD3 nor RD8 indicate such abrupt changes in deposits, we hypothesize that anthropogenic activities along the harbor entrance channel are plausible sources explaining the abrupt changes. Towards the top of core RD1, stress-tolerant species even increase to 45 %. Rising percent abundances in RD1 indicate increasing constraints on the faunal exchange between lagoonal and open-ocean waters and strongly suggest an environmental transition towards present-day conditions with alternating periods of opening and closing of the tidal channel, depending on the strength of tidal currents and shift in littoral drift.

The recent construction of the modern port at the site of the ancient Roman harbor reduced the natural coastal drift and resulted in the accumulation of additional sandy beach sediments south of Rass Dimass, while silting increased towards the north (between the mainland and the sand spit). It is very likely that similar depositional process changes were triggered by the construction of the extensive Roman breakwater mole and have thus been effective since antiquity (Slim et al., 2004).

6 Conclusion

Analyses of micropaleontological and sedimentological data were conducted on three ^{14}C-dated sediment cores to reconstruct the evolution of the Thapsus coastline and the Dzira Lagoon (Tunisia) over the past 4000 years. The proxy records provide evidence for sequences of transgressions that shaped the coastal evolution, the trajectory of depositional facies, the composition of foraminiferal faunal assemblages, and the formation of the Dzira Lagoon. The transgressive events ($\sim$ 4070 and between 2079 and 1280 cal yr BP) are characterized by sandy sediments deposited in a largely open marine lagoon environment and by diverse and species-rich assemblages of shallow-water foraminifera. With rising sea level at approximately 4070 cal yr BP, the shoreline moved to higher grounds. The transgressive sediments overlay marine carbonate sandstones and deposited facies of coarse-grained sands, lithoclasts, and *Posidonia* seagrass debris. Between $\sim$ 4070 and 2273 cal yr BP, offshore bedrock relicts of the Pleistocene shoreline became the focal point for sand accumulations and initiated the formation of a discontinuous barrier, the elongation of the sand spit, and the formation of an open lagoon environment. Foraminiferal faunal assemblages from the newly formed lagoonal environment indicate a reduced marine influence, as indicated by lower species richness values and rising abundances of stress-tolerant taxa (*Ammonia*).

A gradual transition from open to more restricted lagoon conditions from 1280 cal yr BP until the present day is indicated by increasing percent abundances of fine-grained sediments, decreasing species richness values, and lower abundances of typical marine and higher abundances of stress-tolerant taxa. The transition from an open marine to a particularly shallow, semi-enclosed lagoon setting was favored by the formation of an extensive sand spit and the Roman construction of an extensive harbor breakwater mole.

Data availability. The data generated in this study are included within the paper and in Tables 1–2 and Figs. 3–11. Imaged specimens are deposited at the GEOGLOB laboratory, University of Sfax, Tunisia.

Supplement. The supplement related to this article is available online at: https://doi.org/10.5194/jm-41-129-2022-supplement.

Author contributions. MK conceived this research project, processed and analyzed the samples, and performed light microscopy imaging. All authors contributed to fieldwork and sampling. Species identification and SEM imaging were performed by MK and MRL. MK and MRL prepared the paper and figures with contributions from all authors.

Competing interests. The contact author has declared that none of the authors has any competing interests.

Disclaimer. Publisher's note: Copernicus Publications remains neutral with regard to jurisdictional claims in published maps and institutional affiliations.

Acknowledgements. The authors are grateful to Maria da Conceição Freitas and the two anonymous reviewers for their constructive comments and criticism that greatly improved the paper. We thank the editor-in-chief Francesca Sangiorgi and the editors Polina Shvedko and Laia Alegret for helpful suggestions, advice, and editorial assistance.

Review statement. This paper was edited by Laia Alegret and reviewed by Maria Conceição Freitas and two anonymous referees.

References

Anzidei, M., Antonioli, F., Lambeck, K., Benini, A., Soussi, M., and Lakhdar, R.: New insights on the relative sea level change during Holocene along the coasts of Tunisia and western Libya from archaeological and geomorphological markers, Quaternary Int., 232, 5–12, 2011.

Armynot du Châtelet, E., Francescangeli, F., and Frontalini, F.: Definition of benthic foraminiferal bioprovinces in transitional environments of the Eastern English Channel and the Southern North Sea, Rev. Micropal., 61, 223-234, 2018.

Avnaim-Katav, S., Hyams-Kaphzan, O., Milker, Y., and Almogi-Labin, A.: Bathymetric zonation of modern shelf benthic foraminifera in the Levantine Basin, eastern Mediterranean Sea, J. Sea Res., 99, 97–106, 2015.

Bahrouni, N., Bouaziz, S., Soumaya, A., Ben Ayed, N., Attafi, K., Houla, Y., El Ghali, A., and Rebai, N.: Neotectonic and seismotectonic investigation of seismically active regions in Tunisia: a multidisciplinary approach, J. Seismol., 18, 235–256, 2014.

Ben Khalifa, K., Zaïbi, C., Bonnin, J., Carbonel, P., Zouari, K., Mnif, T., and Kamoun, F.: Holocene environment changes in the Hachichina wetland (Gulf of Gabes, Tunisia) evidenced by foraminifera and ostracods, geochemical proxies and sedimentological analysis, Riv. Ital. Paleontol. S., 125, 517–549, 2019.

Bird, C., Schweizer, M., Roberts, A., Austin, W. E. N., Knudsen, K. L., Evans, K. M., Filipsson, H. L., Sayer, M. D. J., Geslin, E., and Darling, K. F.: The genetic diversity, morphology, biogeography, and taxonomic designations of *Ammonia* (Foraminifera) in the Northeast Atlantic, Mar. Micropaleontol., 155, 101726, https://doi.org/10.1016/j.marmicro.2019.02.001, 2020.

Blanc-Vernet, L., Clairefond, P., and Orsolini, P.: Les foraminifères, Géol. Médit., 6, 171–209, 1979.

Bouchet, P. and Rocroi, J. P.: Classification and nomenclator of gastropod families, Int. J. Malacol., 47, 1–397, 2005.

Bouchet, P. and Rocroi, J. P.: Nomenclator of bivalve families with a classification of bivalve families malacologia, Inst. of Malacol., 5, 21–184, 2010.

Buosi, C., Armynot du Châtelet, E., and Cherchi, A.: Benthic foraminiferal assemblages in the current-dominated Strait of Bonifacio (Mediterranean Sea), J. Foramin. Res., 42, 39–55, https://doi.org/10.2113/gsjfr.42.1.39, 2012.

Calvo-Marcilese, L. and Langer, M. R.: Breaching biogeographic barriers: the invasion of Haynesina germanica (Foraminifera, Protista) in the Bahia Blanca estuary, Argentina, Biol. Invasions, 12, 3299–3306, 2010.

Calvo-Marcilese, L. and Langer, M. R.: Ontogenetic Morphogenesis and Biogeographic Patterns: Resolving Taxonomic Incongruences within "Species" of *Buccella* from South American Coastal Waters, Rev. Bras. Paleontol., 15, 23–32, https://doi.org/10.4072/rbp.2012.1.02, 2012.

Carayon, N.: Les ports pheniciens et punique géomorpologie et infrastructure, PhD thesis, Université Strasbourg, 1384 pp., 2008.

Carbonel, P.: Les Ostracodes, traceurs des variations hydrologiques dans les systèmes de transition eau douce eau salée, Mem. Soc. Geol. Fr., 144, 117–128, 1982.

Cimerman, F. and Langer, M. R.: Mediterranean Foraminifera, Slovenska Akademija Znanosti, Ljubljana, 118 pp., 1991.

Dallas, M. F. and Yorke, R. A.: Underwater surveys of North Africa, Jugoslavia and Italy, Underwater Association Report, 21–34, 1968.

Davidson, D. P. and Yorke, R. A.: The Enigma of the Great Thapsus Harbour Mole, Int. J. Naut. Archaeol., 43, 35–40, 2014.

Délibrias, G.: Le carbone 14, in: Méthodes de datation par les phénomènes nucléaires naturels: applications, edited by: Roth, E. and Poty, B., Collection CEA, Éditions Masson, Paris, 421–458, 1985.

Dimiza, M. D., Koukousioura, O., Triantaphyllou, M. V., and Dermitzakis, M. D.: Live and dead benthic foraminiferal assemblages from coastal environments of the Aegean Sea (Greece): distribution and diversity, Rev. Micropal., 59, 19–32, https://doi.org/10.1016/j.revmic.2015.10.002, 2016.

Frezza, V. and Carboni, M. G.: Distribution of recent foraminiferal assemblages near the Ombrone River mouth (Northern Tyrrhenian Sea, Italy), Rev. Micropal., 52, 43–66, 2009.

García-Sanz, I., Usera, J., Guillem, J., Giner-Baixauli, A., and Alberola, C.: Geographical and bathymetric distribution of foraminiferal assemblages from the Alboran Sea (western Mediterranean), Quaternary Int., 481, 146–156, 2018.

Gargouri-Ben Ayed, Z., Souissi, R., Soussi, M., Abdeljaouad, S., and Zouari, K.: Sedimentary Dynamics and Ecological State of Nakta Tidal Flat (Littoral), South of Sfax, Gulf of Gabés, Tunisia, Chin. J. Geochem., 26, 244–251, 2007.

Giocondo, G. and Palladio, A.: Battle of Thapsus, https://commons.wikimedia.org/wiki/File:Battle_of_Thapsus.jpg (last access: 26 August 2022), 1567.

Hammer, Ø., Harper, D. A., and Ryan, P. D.: PAST: Paleontological statistics software package for education and data analysis, Palaeontol. Electr., 4, 9 pp., 2001.

Heaton, T., Köhler, P., Butzin, M., Bard, E., Reimer, R. W., Austin, W. E. N., Ramsey, C. B., Grootes, P. M., Hughen, K. A., Kromer, B., Reimer, P. J., Adkins, J., Burke, A., Cook, M. S., Olsen, J., and Skinner, L. C.: Marine20 - The Marine Radiocarbon Age Calibration Curve (0–55,000 cal BP), Radiocarbon, 62, 779–820, https://doi.org/10.1017/RDC.2020.68, 2020.

Hunt, C. O., Farrell, M., Fenech, K., French, C., McLaughlin, R., Blaauw, M., Bennett, J., Flood, R., Pyne-O'Donnell, S., Reimer, P. J., Ruffell, A., Cresswell, A. J., Kinnaird, T. C., Sanderson, D., Taylor, S., Malone, C., Stoddart, S., and Vellan, N. C.: Chronology and stratigraphy of the valley systems. Temple landscapes fragility, change and resilience of Holocene environments in the Maltese Islands, Mc Donald Institute for Archaeological Research, Cambridge, UK, Vol. 1, 35–71, 2020.

Haunold, T. G., Baal, C., and Piller, W. E.: Benthic foraminiferal associations in the Northern Bay of Safaga, Red Sea, Egypt, Mar. Micropaleontol., 29, 185–210, 1997.

Hayward, B. W., Grenfell, H. R., Reid, C. M., and Hayward, M. R.: Recent New Zealand shallow-water benthic foraminifera: taxonomy, ecologic distribution, biogeography, and use in paleoenvironmental assessment, Institute of Geological & Nuclear Sciences monograph 21, New Zealand Geol. Surv. Paleont. Bull., 21, 1–258, 1999.

Hayward, B. W., Holzmann, M., Pawlowski, J., Parker, J. H., Kaushik, T., and Toyofuku, M. S.: Tsuchiya: Molecular and morphological taxonomy of living Ammonia and related taxa (Foraminifera) and their biogeography, Micropaleontology, 67, 109–313, 2021.

Jedoui, Y., Kallel, N., Fontugne, M., Ben Ismail, M. H., M'Rabet, A., and Montacer, M.: A high relative sea level stand in the middle Holocene of Southeastern Tunisia, Mar. Geol., 147, 123–130, 1998.

Kaminski, M. A., Aksu, A., Box, M., Hiscott, R. N., Filipescu, S., and Al-Salameen, M.: Late Glacial to Holocene benthic foraminifera in the Marmara Sea: implications for Black Sea–Mediterranean Sea connections following the last deglaciation, Mar. Geol., 190, 165–202, 2002.

Kamoun, M., Khadraoui, A., Ben Hamad, A., Zaïbi, C., Langer, M. R., Bahrouni, N., Ben Youssef, M., and Kamoun, F.: Impact of relative sea level change and sedimentary dynamic on an historic site expansion along the coast between Sfax and Jebeniena, Conference of the Arabian Journal Geosciences (CAJG), 12–15 November 2018, Hammamet, Tunisia, 141–143, 2019.

Kamoun, M., Zaïbi, C., Langer, M. R., Khadraoui, A., Ben Hamad, A., Ben Khalifa, K., Carbonel, P., and Ben Youssef, M.: Environmental evolution of the Acholla coast (Gulf of Gabes, Tunisia) during the past 2000 years as inferred from paleontological and sedimentological proxies, Neues Jahrb. Geol. Pal., 296, 217–235, https://doi.org/10.1127/njgpa/2020/0897, 2020.

Kayan, I.: Holocene stratigraphy and geomorphological evolution of the Aegean coastal plains of Anatolia, Quaternary Sci. Rev., 18, 541–548, 1999.

Khadraoui, A., Kamoun, M., Ben Hamad, A., Zaïbi, C., Bonnin, J., Viehberg, F., Bahrouni, N., Sghari, A., Abida, H., and Kamoun, F.: New insights from microfauna associations characterizing palaeoenvironments, sea level fluctuations and a tsunami event along Sfax Northern coast (Gulf of Gabes, Tunisia) during the Late Pleistocene-Holocene, J. Afr. Earth Sci., 147, 411–429, https://doi.org/10.1016/j.jafrearsci.2018.05.011, 2018.

Khadraoui, A., Zaïbi, C., Carbonel, P., Bonnin, J., and Kamoun, F.: Ostracods and mollusks in northern Sfax coast: reconstruction of Holocene paleoenvironmental changes and associated forcing, Geo-Mar. Lett., 39, 313–336, 2019.

Kraft, J. C., Bückner, H., Kayan, I., and Engelmann, H.: The geographies of ancient Ephesus and the Artemision in Anatolia, Geoarchaeology, 22, 121–149, https://doi.org/10.1002/gea.20151, 2007.

Lakhdar, R., Soussi, M., Ben Ismail, M. H., and M'Rabet, A.: A Mediterranean Holocene restricted coastal lagoon under arid climate: case of the sedimentary record of Sabkha Boujmel (SE Tunisia), Palaeogr. Palaeocl., 241, 177–191, 2006.

Langer, M. R.: Recent epiphytic foraminifera from Vulcano (Mediterranean Sea), Rev. Paléobiol., 2, 827–832, 1988.

Langer, M. R.: Distribution, Diversity and Functional Morphology of Benthic Foraminifera from Vulcano (Mediterranean Sea), PhD thesis, University of Basel, 159 pp., 1989.

Langer, M. R.: Epiphytic foraminifera, Mar. Micropal., 20, 235–265, https://doi.org/10.1016/0377-8398(93)90035-V, 1993.

Langer, M. R. and Schmidt-Sinns, J.: The 100 most common Foraminifera from the Bay of Fetovaia, Elba Island (Mediterranean Sea), Monographie im Selbstverlag, Institut für Paläontologie, Universität Bonn, 1–15, 2006.

Langer, M. R., Hottinger, L., and Huber, B.: Functional morphology in low-diverse benthic foraminiferal assemblages from tidal-flats of the North Sea, Senck. Marit, 20, 81–99, 1990.

Langer, M. R., Frick, H., and Silk, M. T.: Photophile and sciaphile foraminiferal assemblages from marine plant communities of Lavezzi Islands (Corsica, Mediterranean Sea), Rev. Paléobio., 17, 525–530, 1998.

Langer, M. R., Thissen, J. M., Makled, W. A., and Weinmann, A. E.: The foraminifera from the Bazaruto Archipelago (Mozambique), Neues Jahrb. Geol. Pal., 297, 155–170, https://doi.org/10.1016/j.revmic.2009.11.001, 2013.

Masmoudi, S., Yaich, C., and Ammoun, M.: Evolution et morphodynamique des iles barrières et des flèches littorales associées

à des embouchures microtidales dans le Sud-Est tunisien, Bull. l'Inst. Sci., Section Sciences de la Terre, 27, 65–81, 2005.

Mateu-Vicens, G., Box, A., Deudero, S., and Rodríguez, B.: Comparative analysis of epiphytic foraminifera in sediments colonized by seagrass *Posidonia oceanica* and invasive macroalgae *Caulerpa* spp., J. Foramin. Res., 40, 134–147, 2010.

Morhange, C. and Pirazzoli, P. A.: Mid-Holocene emergence of southern Tunisian coasts, Mar. Geol., 220, 205–213, 2005.

Morigi, C., Jorissen, F. J., Fraticelli, S., Horton, B. P., Principi, M., Sabbatini, A., and Negri, A.: Benthic foraminiferal evidence for the formation of the Holocene mud-belt and bathymetrical evolution in the central Adriatic Sea, Mar. Micropaleontol., 57, 25–49, 2005.

Morzadec-Kerfourn, M. T.: L'évolution des Sebkhas du Golfe de Gabès (Tunisie) à la transition Pléistocène supérieur – Holocène, Quaternaire, 13, 111–123, 2002.

Murray, J.: Ecology and applications of benthic foraminifera, Cambridge University Press, 426 pp., https://doi.org/10.1017/CBO9780511535529, 2006.

Oflaz, S. A.: Taxonomy and distribution of the benthic foraminifera in the Gulf of Iskenderun, Eastern Mediterranean, MSc thesis, Middle East Technical University, http://etd.lib.metu.edu.tr/upload/3/12607725/index.pdf (last access: 26 August 2022), 2006.

Oueslati, A.: Les côtes de la Tunisie: géomorphologie et environnement et aptitudes à l'aménagement, Publications de l'Université de Tunis, Faculté des Lettres et Sciences Humaines, 34, 387 pp., 1993.

Paskoff, R. and Sanlaville, P.: Les côtes de la Tunisie. Variations du niveau marin depuis le Tyrrhénien, 14, 1, Persée-Portail des revues scientifiques en SHS, 1983.

Pielou, E. C.: The measurement of diversity in different types of biological collections, J. Theor. Biol., 13, 131–144, 1966.

Saad, S. A. and Wade, C. M.: Biogeographic distribution and habitat association of *Ammonia* genetic variants around the coastline of Great Britain, Mar. Micropaleontol., 124, 54–62, 2016.

Sgarrella, F. and Moncharmont Zei, M.: Benthic foraminifera of the Gulf of Naples (Italy): systematics and autoecology, Boll. Soc. Paleontol. I., 32, 145–264, 1993.

Siani, G., Paterne, M., Arnold, M., Bard, E., Metivier, B., Tisnerat, N., and Bassinot, F.: Radiocarbon reservoir ages in the Mediterranean Sea and Black Sea, Radiocarbon, 42, 271–280, 2000.

Slim, P., Trousset, P., Paskoff, R., and Oueslati, A.: Le littoral de la Tunisie, Et. Géoarch. Hist., CNRS, 185–187, 2004.

Souissi, R., Turki, I., and Souissi, F.: Effect of submarine morphology and environment quality: Case of Monastir Bay (Eastern Tunisia), Carpath. J. Earth Env., 9, 231–239, 2014.

Vita-Finzi, C. and Roberts, N.: Selective leaching of shells for ^{14}C dating, Radiocarbon, 26, 54–58, 1984.

Yorke, R. A.: Les ports engloutis de Tripolitaine et de Tunisie, Archeologia, 17, 18–24, 1967.

Younes, A.: L'installation portuaire à Thapsus: mise au point à partir des textes anciens et de la documentation archéologique, La Méditerranée: l'Homme et la mer, Actes du premier séminaire, Mahdia décembre 1998, CERES, Tunis, 21, 181–193, 1999.

Zaïbi, C., Kamoun, F., Viehberg, F., Carbonel, P., Jedoui, Y., Abida, A., and Fontugny, M.: Impact of relative sea level and extreme climate events on the Southern Skhira coastline (Gulf of Gabes, Tunisia) during Holocene times: Ostracodes and foraminifera associations response, J. Afr. Earth Sci., 118, 120–136, 2016.